ADMINISTRATIVE

RECIPIENT
Sara Hotchkiss, Associate professor, shotchkiss@wisc.edu, 608-265-6751

RECIPIENT INSTITUTION
University of Wisconsin-Madison, Botany Dept., 430 Lincoln Drive, Madison, WI 53706

PROJECT TITLE
Predicting future distribution of cloud forest and high-elevation species in Hawai‘i: integrating modern and paleoecological data to plan for climate change

FWS AGREEMENT NUMBER
12170-B-G100

RECIPIENT ID NUMBER
144-PRJ51YC

REPORT DATE
December 31, 2014

REPORT AUTHOR
S. Crausbay

REPORT PERIOD
August 2011 – December 2014

TOTAL COST
$91,785.00

PUBLIC SUMMARY

This study focused on sensitivity of high-elevation ecosystems in Hawai‘i to climate change. These Hawaiian ecosystems are becoming warmer and drier, and are relevant because they house many rare species, represent the last remaining stretches of uninvaded landscapes, and include *wao akua* – the small-statured cloud forests of great cultural significance that are the ‘realm of the gods’. Rapid climate change here presents a disproportionately high climate change impact risk. We provided models that relate current, past, and future distribution of plant species from 6000 – 7500’ feet in elevation on Haleakalā, to mean climate, extreme drought events, and soil properties. We constructed 24 models of current vegetation and found that moisture – both overall mean moisture and moisture during an El Niño drought event – was a strong driver of vegetation patterns today; whereas temperature and soils were less important. We tested whether El Niño frequency was related to changes in vegetation over very long time scales with paleorecords of the forest’s upper limit and climate that extend over 3000 years. We found that indeed, the upper limit of forest shifted up or down the mountain depending on the frequency of El Niño drought events (downslope shift with greater drought frequency) and local moisture availability. We analyzed the sensitivity of vegetation to future changes in rainfall – from a 30% reduction in rainfall to a 30% gain. We found that vegetation is often more sensitive to reduced rainfall than to an equal amount of increased rainfall. With reduced rainfall, vegetation tends to move downslope. These data establish the importance of moisture and El Niño to high-elevation ecosystems and cast doubt on a common expectation of upslope movement of vegetation with warming in Hawai‘i. Downslope movement of vegetation with reduced moisture is an important scenario for planning and management. However, the future of El Niño, which is largely unknown, may also be important for predicting future vegetation changes.

PROJECT REPORT

TECHNICAL SUMMARY

This study’s goal was to focus on ecological responses to climate change at high elevations in Hawai‘i. These Hawaiian mauka ecosystems are particularly vulnerable to climate change because warming is amplified at high elevations and the trade wind inversion (TWI) is changing in ways that enhance aridity. Mean TWI position is highly relevant ecologically because abrupt changes in humidity and precipitation at the TWI coincide with an abrupt ecotone between cloud forest and subalpine shrublands. Ecosystems around the TWI are relevant because they house an incredible array of endemic species, represent some of the last uninvaded landscapes, and include culturally significant lands. This project offers current, past, and future species and habitat distribution models for vegetation around the TWI. We assessed the sensitivity of vegetation around the TWI on Haleakalā to climate change with high-resolution habitat and species distribution models (SDMs) driven by soils, mean climate, and climate during El Niño-induced drought. For those vegetation models driven by rainfall, we modelled future abundance and distribution based on statistically downscaled rainfall projections (Timm et al. 2014). We also modelled past forest line dynamics with SDMs built from paleorecords to test understandings based on present and future SDMs.

We constructed 24 baseline (current) distribution models testing the relative importance of non- El Niño climate, climate during an El Niño (EN) drought event, and substrate characteristics – aspect, percent slope, and substrate age and texture. Moisture was important in more than half (16) of all models but temperature was important in less than half (9). We found that climate during EN was important in many models (11) and the importance value for relative

humidity during EN across all models was not significantly different from that of temperature, rainfall, or relative humidity during non-EN climate. Vegetation at and above the TWI was driven by EN more often than vegetation below the TWI. The position of the cloud forest's upper limit is one such vegetation model driven by EN. We tested whether forest line dynamics were associated with EN in the past with 3300-year long paleorecords of forest line and climate. We found that forest line moved upslope with reduced frequency of EN droughts and downslope with increased EN frequency. We constructed future models for vegetation characteristics driven by rainfall by using PICCC-supported statistical downscaling products for rainfall in Hawai‘i (Timm et al. 2014). We found that distribution of cloud forest and the tussock grass *Deschampsia nubigena* moves downslope with decreased rainfall but is less sensitive to increased rainfall. Overall, vegetation here is strongly associated with mean climate, especially moisture, and climate during El Niño-induced drought. Downslope movement of vegetation with reduced moisture, rather than the commonly expected upslope movement with warming, is an important scenario for planning and management around the TWI. However, the future of El Niño, which is largely unknown, may be more important for predicting future forest line and other vegetation changes. These PICCC-funded research accomplishments contribute to scientific knowledge and regional climate change adaptation by (1) highlighting the role of extreme climatic events (i.e., El Niño) in ecosystem response to climate change and (2) integrating past, present, and future distribution models to understand ecosystem sensitivity to climate change.

PURPOSE AND OBJECTIVES

This project addressed issues of vegetation sensitivity at high elevations around the TWI in Hawai‘i. Study of climate-change sensitivity here has important implications for both conservation and water availability. Hawai‘i's high-elevation cloud forest is the last remaining intact habitat for many endangered forest bird species threatened by non-native avian malaria. As temperature increases, malaria will move uphill. Study of forest line ecotone climate-change sensitivity has important implications for forest bird conservation planning specifically. Will cloud forest move uphill in response to warming, or downhill in response to increased aridity? The answer will inform decisions, for example, about whether to restore high-elevation forests on Mauna Kea lost to grazing. These high-elevation closed-canopy forests also absorb and store vast amounts of rainfall, and thus provide immense supplies of water to downstream users, including indigenous and conventional agriculture. This research highlights the potential for forest line to change elevation, which has implications for total cloud forest area, and thus total watershed yield.

We began this project with four major objectives:

1) We will use PICCC-supported downscaling products ("Climate Change Impacts on Critical Ecosystems in Hawai‘i and US Pacific Islands Territories" Timm et al.) and a recent study linking vegetation patterns to moisture availability to provide species and habitat distribution models for future rainfall and temperature surfaces near the TWI on the NE corner of Haleakalā volcano. Models will focus on the distribution of cloud forest habitat and the abundance of important indicator taxa, such as *Metrosideros polymorpha*, epiphytes, invasive species, and other taxa of management concern.

2) We will use forthcoming CMIP5 future climate projections and retrospective datasets that relate ~3,300 years of vegetation change with fire, onsite drought, ENSO frequency, mean latitude of the Intertropical Convergence Zone (ITCZ), and the PDO and the Aleutian Low

to develop a second set of distribution models that highlight how vegetation responds to longer modes of climate variability and the importance of fire.

3) We will help convene a workshop – "Holocene paleoclimate in the Hawaiian Islands and its large-scale context" – led by Henry Diaz, to bring together leading climatologists and paleoclimatologists working in the Pacific Basin. Primary goals of the workshop are to evaluate paleoclimatic records, assess causal links between climate patterns in the Pacific, highlight needs for further research, and explore areas of collaboration.

4) We will maintain a climate network, Little HaleNet, that is integrated with permanent vegetation plots and the older climate network, HaleNet.

We completed most of these objectives and are nearly complete with others:

Product	**Expected Date**	**Actual Date**	**Status**
Workshop on paleoclimate in Hawai'i and the Pacific	November 2011	November 7-8, 2011	Complete
Current distribution models, publication	January 2012	January 2014	Complete – published in Oecologia
Paleo-distribution models, publication	September 2013	Estimated March 2015	Manuscript in preparation, draft shared with PICCC
Paleoclimate in Hawai'i and the Pacific, technical report	September 2013	Estimated January 2015	Report in preparation
Future distribution models I, publication	April 2014	Estimated May 2015	Preliminary analysis complete presented in PICCC webinar Sept 2014
Future distribution models II, publication	April 2014	NA	Too much uncertainty in the future of ENSO to complete this task
Paleorecords of upper forest response to drought and fire, publication	Additional product; not initially proposed	November 2014	Published in Arctic, Antarctic, and Alpine Research in a special feature on tropical alpine ecosystems
Maintenance of Little HaleNet climate array	Ongoing	Ongoing	Ongoing

There was too much uncertainty in the future of EN to complete "Future distribution models II", where we proposed to use the past distribution model of dynamics in forest line with changes in EN frequency to consider the future forest line with future EN scenarios. We focused instead on gathering more data from paleorecords. We published analysis on the response of upper cloud forest to drought and

fire over the past 7000 years in a special feature on tropical alpine ecosystems in Arctic, Antarctic, and Alpine Research.

ORGANIZATION AND APPROACH

Baseline distribution models

Response variables

Vegetation structure and composition were quantified in 136 plots which comprise 15-m long transects that were established along nine elevational transects with a stratified random approach (Crausbay and Hotchkiss 2010). The point-intercept method (Levy and Madden 1933) was used to quantify species presence every 25 cm along each data transect, in five height classes (0–1 m, 1–2 m, 2–3 m, 3–5 m, and > 5 m). All vascular plants were identified to the species or variety level, but bryophytes and lichens were not differentiated further. Forest line position was defined by the sharp discontinuity where the > 5 m height class dropped from > 60% cover to < 25% cover in successive plots (Crausbay and Hotchkiss 2010). The > 5 m height class was chosen because trees near the forest line on Haleakalā are 5 to 8 m tall (Kitayama and Mueller-Dombois 1992).

Baseline distribution models include 24 different vegetation response variables, including species abundance, forest line position (binary), the abundance of the > 5m height class, and community metrics based on ordination (Table 1). We used the primary axis from a non-metric multi-dimensional scaling (NMS) ordination with a Sørensen distance matrix 2w/(a + b), where a and b are the numbers of species in each of two samples and w is the number of species common to both samples. The ordination was performed in PC–ORD™ 6.0 (MjM Software Designs, Gleneden Beach, OR, USA).

Predictor variables

Microclimate data were obtained from 15 stations – three within the HaleNet climate network and all 12 of the Little HaleNet (LHN) climate network. LHN uses HOBO® Micro Station Data Loggers (H21-002, Onset Computer Corporation, Massachusetts, USA) to record temperature at 0.02°C resolution and ± 0.21°C accuracy and relative humidity at 0.01% resolution and ± 2.5% accuracy (S-THB-M002, since 2008), and rainfall with a stainless steel tipping bucket at 0.2-mm resolution and ± 1% accuracy (RG2-M, since 2005). The remaining three stations from the HaleNet network measure, among other variables, temperature (±0.4 °C accuracy) and relative humidity (± 2.5% accuracy) with a Vaisala (Helsinki, Finland) HMP45C probe and rainfall with a Texas Electronics (Dallas, TX, USA) model TE525 tipping-bucket rain gage at 0.254-mm resolution.

Hourly data for rainfall (mm), relative humidity (%), and temperature (°C) were aggregated into monthly values for August 2005 – July 2010. Seasonal – December-February (DJF), March-May (MAM), June-August (JJA), and September-November (SON) – and annual means (sums in the case of rainfall) were calculated from the monthly data. In addition, average number of consecutive rainless days and total number of rainless days for each station were calculated. Total number of rainless days was expressed as a per-year value (normalizing by the number of days of observation out of 365 days). Freezing air temperatures are rare near the forest line (Kitayama and Mueller-Dombois 1992) and since 2005 the lowest temperature recorded there was 0.7°C. Frost damage in leaves of the primary canopy tree, *Metrosideros polymorpha*, occurs at -8.5°C or lower (Melcher et al. 2000). Therefore, the influence of freezing temperatures on the forest line position was not considered further.

High-resolution (5 m) gridded climate surfaces were generated from the 15 climate stations' data with ordinary kriging using the Geostatistical Analyst extension in ArcGIS™ 10 (ESRI, Redlands, CA, USA). Kriging takes advantage of the spatial correlation between stations and is widely used for interpolating climate variables. Kriging can incorporate secondary variables, but in Hawai'i, the use of a secondary variable does not improve the interpolation for rainfall (Frazier 2012). Ordinary kriging has been shown to outperform Thiessen polygons, inverse distance weighting, linear regression, ordinary co-kriging, kriging with external drift, and simple kriging with varying local means (Mair and Fares 2011; Frazier 2012). Ordinary kriging's better performance is related to the complex mechanisms affecting climate in Hawai'i that make it difficult for one covariate to improve the prediction. In fact, some covariates such as elevation are particularly inappropriate at high elevations in Hawai'i because of the TWI, a shifting temperature inversion. In addition, station density in this study (3.5 stations km^{-2}) is much greater than in previous studies that have tested interpolation methods for rainfall in Hawai'i (range of rain gauge densities = 0.125 – 0.23 stations km^{-2}; Mair and Fares 2011; Frazier 2012), reducing the need for secondary variables. To reduce bias in this analysis that could be introduced by using multiple interpolation methods for the different variables, a single method (ordinary kriging) was used to interpolate all variables (e.g., Letten et al. 2013).

Microclimate predictor variables were extracted from the gridded surfaces at each of the 136 vegetation plots and include three groups – air temperature, relative humidity, and rainfall – from (i) non-El Niño periods and (ii) a strong El Niño winter. There were no strong La Niña winters during this study period. For non-El Niño periods, each group of predictor variables includes annual and seasonal data 2005-2010 for rainfall and 2008-2010 for relative humidity and temperature. We defined a strong El Niño event when the mean for the Multivariate ENSO Index (MEI, Wolter and Timlin 2011) ranks for any three-month season fell within the 10th percentile. The MEI is defined by multivariate characteristics and allows for spatial variations and historical definitions of ENSO in the instrumental record, unlike other ENSO indices (e.g., Niño3.4; Wolter and Timlin 2011). Microclimatic data during seasons that the MEI ranks classified as neutral, weak El Niño, and weak La Niña, based on the 10th percentile definition for strong events, are all considered non-El Niño periods in this study, as weak El Niños or La Niñas are not associated with strong climate anomalies in Hawai'i (da Silva 2012). Climate variables during these non-El Niño periods were highly correlated with each other within a particular group (e.g., rainfall). The mean Pearson's r between all pairwise total rainfall variables = 0.96, mean relative humidity variables = 0.95, and mean temperature variables = 0.89.

To minimize the effects of collinearity in predictor variables and avoid model over-fitting, only one predictor was selected to represent total rainfall, mean relative humidity, and mean temperature during the non-El Niño periods. Selections were made through a screening process in a non-parametric multiplicative regression (NPMR) in HyperNiche 2.0 (MjM Software Designs, Gleneden Beach, OR, USA). NPMR screens predictors individually by seeking the best fit between the response and each predictor, one at a time, with a kernel smoothing function. Models were selected based on the best mean goodness of fit after incorporating a leave-one-out cross-validation. For quantitative models, fit was evaluated with a cross-validation procedure, a cross R2 (xR2). For binary models, fit was evaluated with logB, the log10 of likelihood ratio and area under the receiver operating characteristic curve (AUC). The microclimate variable with the best fit was used to represent the non-El Niño periods for that group (e.g., rainfall).

Microclimate characteristics during the strong El Niño winter differ significantly from those during non-El Niño periods (Wilcoxon signed rank test; relative humidity P = 0.01, rainfall P = 0.008, temperature P = 0.03; Fig. 2). Our 15-station climate network captured the strong El Niño during the winter of 2009-2010, which agrees broadly with the five other strong El Niño winters measured at the forest line over the past 20 years (Fig. 2). We used total rainfall, mean relative humidity, and mean temperature from the 3-month winter season (DJF) 2009-2010 to represent a strong El Niño event. In Hawai‘i, strong El Nino's tend to impact the entire winter season (Chu 1989; Chu and Chen 2005), so we focus on mean or total microclimate characteristics during this time period.

Substrate characteristics were also included as predictor variables. We measured percent slope and plot orientation (aspect) in each vegetation plot. We used a digital geological map (Sherrod et al., 2007) to define substrate age and texture for each plot.

NPMR distribution modeling

Habitat models use 10 predictor variables: total rainfall, mean relative humidity, and mean temperature representing non-El Niño periods; total rainfall, mean relative humidity, and mean temperature from the strong El Niño winter of 2009-2010; and percent slope, substrate age, aspect, and soil texture. We used NPMR to construct models. NPMR searches all possible permutations of model possibilities for a full optimization. Estimated response for a particular predictor was determined by a local mean model and a weighted Gaussian kernel function, which weights points closer to the target more heavily. Over-fitting is constantly controlled in NPMR through built-in cross-validation. In addition, we set the improvement criterion at 5%, the data:predictor ratio minimum at 5, and the minimum average neighborhood size, N*, at 3% of sites, where N* is the average sum of the weights for other data points that bear on the target point. Models were selected based on the best cross-validated fit with the lowest number of predictor variables after incorporating a leave-one-out cross-validation. Fit was evaluated as described above for NPMR's screening process for microclimate predictor variables (xR2 for quantitative models; logB and AUC for the binary forest line model). Model significance was determined for the highest evaluated model with P, the results of a 1000-run Monte Carlo randomization test.

We compared the variable importance of mean climate, El Niño climate, and substrate. Sensitivity of the model to each predictor was measured by nudging the values up and down by 5% of the range of individual predictors, and calculating the resulting change in the estimate for that point (McCune 2006). Sensitivity measures we report are the mean absolute difference resulting from nudging the predictors and are expressed as a proportion of the range of the response variable. Sensitivity measures are independent of variable units and higher sensitivities represent more important predictor variables.

We chose NPMR as a preferred algorithm because it allows predictor variables to interact – a more realistic approach to ecological modeling (McCune 2006). NPMR is similar to a generalized additive model (GAM) with smoothing functions, but it combines predictor variables multiplicatively and automatically models interactions with a multiplicative kernel function, rather than requiring that interactions among predictors be specified explicitly. NPMR is flexible and can model both quantitative and binary response variables. We tested the robustness of NPMR results of our binary forest line model, showing that relative humidity during El Niño was the strongest driver, with Boosted Regression Trees, Random Forests, Multivariate Adaptive Regression Splines, and a Generalized Linear Model. We found that relative humidity during El

Niño was also the most important variable in all but Boosted Regression Trees, where it was the second most important variable.

Future distribution models

Response variables

We modelled the future of vegetation characteristics that were driven, at least in part, by rainfall. These models included the abundance of *Deschampsia nubigena*, *Myrsine lessertiana*, Bryophytes, vegetation >5m, the forest line position, and overall community composition in the cloud forest (axis 1 of a NMS ordination).

Future rainfall scenarios

We extracted future rainfall data for each vegetation plot using statistical downscaling products based on the CMIP5 Global Model Projections (Elison Timm et al. 2014). This downscaling product uses the median from 32 downscaled GCMs and two different representative concentration pathways (8.5 and 4.5) to project dry and wet season rainfall. We use the mid-century scenarios for RCP 8.5 and RCP 4.5. We also added additional scenarios to balance the degree of rainfall change more equally, in order to interpret model results in terms of vegetation sensitivity. In our baseline dataset, climate variables during non-El Niño periods – be they individual months, dry or wet seasons, or annual means – were highly correlated with each other within a particular group (e.g., rainfall). The mean Pearson's r between all pairwise total rainfall variables = 0.96, mean relative humidity variables = 0.95, and mean temperature variables = 0.89. As a result, even if a baseline model was driven by wet season rainfall, we modelled the future scenarios based on statistical downscaling of both wet and dry season rainfall. Our data are meant to be interpreted in terms of vegetation sensitivity, not in terms of a precise vegetation future.

Differences in abundance/distribution

To determine whether and how future rainfall changes affect abundance, we performed paired t-tests, or Wilcoxon Signed Rank tests when our data failed a Shapiro-Wilk normality test, on each projected future's abundance compared to the current (baseline) abundance. To determine how rainfall changes affect distribution, we mapped abundances from each future rainfall scenario.

Past distribution models

Response variables

Vegetation-pollen relationships were analyzed by collecting soil samples, which serve as a modern pollen calibration library, from vegetation plots. Recent work calculated several metrics from these soil samples' pollen assemblages and applied the receiver operator characteristic (ROC, e.g., Metz 1978) to compare metric performance at distinguishing vegetation around the upper forest line (Crausbay & Hotchkiss 2012). This work showed the sum of taxa indicative of either subalpine-alpine ecosystems or cloud forest was the most accurate predictor of forest line. The percentage of subalpine-alpine indicators was used as the response variable to represent forest line position.

Predictor variables

Habitat models use 3 predictor variables: El Niño frequency (Moy et al. 2008), onsite hydrology (delta-D of leaf waxes) and position of the Intertropical Convergence Zone (Haug et al. 2001). We used NPMR to construct distribution models, as above.

Other paleorecords

Coring & chronology

We recovered sediment sequences from Flat Top Bog and the two lakes Wai‘ele‘ele and Wai‘ānapanapa with a modified Livingstone piston corer. Cores were split longitudinally into working and archived halves, photographed, described, and subjected to magnetic susceptibility analysis. The working halves of sediment cores were sliced into 0.5-cm intervals. Dating control was provided by several Accelerator Mass Spectrometer (AMS) ^{14}C measurements on terrestrial plant material, including leaves, stems, seeds, wood, and pollen/spore concentrates that were obtained with heavy liquid separation (Table 1). Radiocarbon dates were calibrated with IntCal09, converted to cal yr Before Present (BP), where “present” is 1950 C.E., and age-depth models were constructed using the Bayesian techniques in the P_Sequence algorithm in OxCal v4.1.7 software with k = 1 cm (Bronk Ramsey, 2009).

Pollen

We subsampled 1 cm^3 of sediment to concentrate pollen/spores using standard techniques including acetolysis (Faegri and Iversen, 1989). Pollen/spore residues were mounted in silicone oil and all pollen and fern spores were quantified at 400x and sometimes 1000x until we reached a sum of 500 pollen grains (excluding any fern spores). Pollen and spore percentages were then calculated from raw counts after psilate monolete fern spores and wetland taxa (Poaceae, Cyperaceae, Tubuliflorae undifferentiated, *Plantago*) were excluded from the sum (after Crausbay and Hotchkiss, 2012).

Charcoal

We reconstructed the fire regime with a contiguous record of microscopic charcoal fragments. Influx of small fragments of charcoal records the occurrence of past fires and both theoretical and empirical studies demonstrate that charcoal > 125 μm provides the best indication of local fires (methods reviewed in Whitlock and Larsen, 2002). We quantified charcoal particles > 125 μm in contiguous 0.5-cm increments of the sediment core. For each sample, we processed 1 cm3 of sediment by treating with hot 10% KOH, sieving, transferring material > 125 μm to a petri dish, and ‘bleaching’ the sample with 30% H2O2 in a drying oven at 60°C for 24 hours. We counted charcoal particles at 60x magnification on a dissecting microscope.

Biomarkers

We reconstructed the drought regime with the abundance of sedimentary n-alkanes from Wai‘ānapanapa, which sits at the modern forest line. Sedimentary n-alkanes were calibrated by modern samples across an elevational gradient. The modern samples focused on two types of *Metrosideros polymorpha* leaves – a glabrous variety (var. *microphylla*) abundant at lower elevations in wetter areas and pubescent varieties (var. *polymorpha* and var. *incana*) abundant at higher elevations in drier areas. The modern leaf sites include (1) four pubescent and three glabrous sites taken along an elevational gradient from ~ 100 m to 2400 m a.s.l. on the windward, east slope of Mauna Loa volcano on the Island of Hawai‘i (Kahmen et al., 2011), and (2) two pubescent sites near the modern TWI on the windward side of the island of Maui at 2040

m and 2090 m. Alkanes were analyzed on 27 samples, which included several *M. polymorpha* leaves from three trees at each of the nine sites. Since leaf wax composition was very similar among the replicates (three trees per site), we report only mean site average chain length (ACL) of n-alkanes here (standard deviations for the ACL ranged between 0.17 and 0.69, with a mean standard deviation of 0.41).

This modern library of *M. polymorpha* n-alkanes aids the interpretation of n-alkanes on samples from the sediment core. To measure sedimentary n-alkanes, we took 48 subsamples of 5 cm3 of sediment on average every 11 cm. All alkanes were extracted in the organic geochemical laboratory at University of Potsdam, Germany using an accelerated solvent extraction system (ASE 350, Dionex Corp, Sunnyvale, USA) to obtain total lipid extracts. Total lipid extracts were further separated using silica gel chromatography (solid phase extraction, SPE) into three fractions: hydrocarbons (containing the n-alkanes), alcohols and fatty acids. The first fraction containing the n-alkanes were analyzed using an Agilent 7890A Gas Chromatograph (GC) with an Agilent 5975C mass spectrometric detector (MSD) to identify and with a flame ionization detector (FID) (Agilent Technologies, Palo Alto, USA) to quantify biomarkers; the other fractions were archived. A more detailed description of the n-alkane extraction procedure and GC-MSD/FID measurement is given elsewhere (Garcin et al., 2012). Peak areas of nC25 to nC33 alkanes were obtained from the FID detector trace for the calculation of the average chain length values.

Data analysis – vegetation dynamics at the upper limit of forest

To assess overall stability of vegetation, we conducted rate-of-change analysis with the Sørensen distance metric, 2w/(a + b), where w is the sum of shared abundances and a and b are the sums of abundances in individual sample units, to quantify the dissimilarity between all adjacent pollen/spore spectra (McCune and Grace, 2002). We divided the resulting dissimilarity index, expressed as percentages where values range from 100% (no species in common) to 0% (identical species composition) by the number of years elapsed between samples (e.g., Cole, 1985; Gavin et al., 2013). This analysis was performed in PAST™ 2.17c (Hammer et al., 2001; can be accessed at http:folk.uio.no/ohammer/past).

To assess variation in vegetation community composition, pollen percentages were subjected to nonparametric multidimensional scaling (NMS). Variance explained was distributed among the primary axes by calculating the coefficient of determination (r2) between distances in the ordination space and distances in the original space. Ordinations were based on a Sørensen distance matrix. Correlations between an individual taxon's abundance and axis scores were assessed with a Pearson's r. All of these analyses were performed in PC–ORD™ 6.0 (MjM Software Designs, Gleneden Beach, OR, USA).

Data analysis – fire regime at the upper limit of forest

We reconstructed local fire events and fire return interval by separating charcoal accumulation curves into a low frequency 'background' component and a high frequency 'peak' component. Charcoal concentration was first interpolated to the median sample interval of 2.5 years and smoothed using LOWESS with a window width of 300 years (Higuera et al., 2009). Peaks most likely to represent local fires were identified in CharAnalysis as Cpeak = Cinterpolated – Cbackground, with a locally defined threshold level with a 300-year window and a Gaussian mixture model that fits two overlapping distributions to the peak frequency distribution for the sediment core. Threshold values that identify a peak, and thus a fire event,

were determined as a percentage of the noise distribution, with only peaks >99.9% of the noise distribution retained for peak analysis and calculation of fire return intervals. Peaks were discarded if the minimum charcoal particle count within 75 years of a peak had a >5% chance of coming from the same Poisson distribution as the maximum peak sample count. Peaks that passed both the threshold and the minimum count test were used to calculate fire return interval. We used the program CharAnalysis, written by PE Higuera and freely available at https://sites.google.com/site/charanalysis/. We compared charcoal accumulation rates three periods of the Wai‘ānapanapa record with contrasting rates of charcoal accumulation with a Kruskal-Wallis one way analysis of variance (ANOVA) on ranks and conducted a pairwise multiple comparison procedure using Dunn's Method; all performed in SigmaPlot™ version 12.0 (Systat Software, San Jose, CA).

Data analysis – moisture at the upper limit of forest

We used peak areas of nC25 to nC33 alkanes for the calculation of the ACL index using the following equation:

$$ACL=\Sigma n*area(Cn)/\Sigma area(Cn),$$

where n is number of carbon atoms of the alkane and area(Cn) the appropriate area of the compound with n carbon atoms.

We compared the sedimentary paleorecord of ACL to the sediment surface sample, interpreted in a context of n-alkane concentration and ACL of modern *M. polymorpha* leaf samples. Drought is defined as a time period when samples frequently showed ACL lower than the sediment surface sample, because the site is currently situated at the modern mean TWI on a steep moisture gradient. These samples likely originated from a greater abundance of the pubescent *M. polymorpha* variety, suggesting drier conditions and a TWI below Wai‘ānapanapa.

Data analysis – vegetation and disturbance at the upper limit of forest

To show the relationship between disturbance and vegetation in Wai‘ānapanapa, we first categorized each pollen sample based on evidence of fire (defined by charcoal), evidence of drought (defined by ACL), and evidence of dieback (defined by samples with < 35% tree pollen and scores < -1.2 on axis 2, see Results). We quantified whether species composition was significantly different in samples associated with a particular type of disturbance (e.g., drought vs. no drought, fire vs. no fire, and dieback vs. no dieback), with a multi-response permutation procedure (MRPP), a nonparametric method for testing multivariate differences among pre-defined groups. We used a Sørensen distance measure and a weighting option for each item in the group = n(I)/sum(n(I)). MRPP provides a chance-corrected within-group agreement value, A = 0 when heterogeneity within groups equals expectation by chance; A > 0 with more heterogeneity within groups than expected by chance. We identified the taxa that were correlated with a particular disturbance type with Indicator Species Analysis (ISA) based on Dufrêne and Legendre’s (1997) method. We also identified species composition groups, independent of disturbance type, with hierarchical agglomerative clustering (flexible beta = -0.25 linkage method based on a quantitative Sørensen distance matrix, McCune and Grace, 2002) and stratigraphically unconstrained pollen assemblage data. To visualize the relationship between vegetation and disturbance, we overlaid these independently derived species composition groups on the ordination, along with disturbance ellipses. All of these analyses were performed in PC–ORD™ 6.0.

PROJECT RESULTS

Baseline distribution models

Across all of our baseline (current) models, we found that a significant portion (67%) of vegetation response variables (e.g., abundance of species x, forest line position, etc.) were driven by moisture (either rainfall or relative humidity) and only 38% were driven by temperature (Table 1). Nearly half (46%) of all baseline models were driven by climate patterns during El Niño. El Niño-driven vegetation models were common in alpine and subalpine vegetation including (1) three of four forest line models, (2) community composition above forest line, (3) alpine grassland invasive species (*Hypochaeris radicata* and *Holcus lanatus*), (4) *Sadleria cyatheoides* the subalpine shrubland dominant, and (5) *Cheirodendron trigynum*, which along with ohia, is the only other tree that forms the tree line. The abundance of standing dead litter is also modeled with EN, suggesting past mortality events may have been driven by EN-induced drought, especially in wet, eastern areas.

Vegetation Response Variable	Fit (xr^2 or AUC)	Predictor Variables Sensitivity Analyses								
		Temp	RH	Rain	EN-T	EN-RH	EN-R	Slope	Age	Aspect
Forest line$_{sub_height}$	0.58	0.59		0.24		1.03				
Forest line$_{all_height}$	0.60		1.29							
Forest line$_{sub_binary}$	0.98 (AUC)			0.5		1.39				
Forest line$_{all_binary}$	0.99 (AUC)	0.44				1.30				
Community$_{all}$	0.90	0.66	0.61							
Community$_{above}$	0.78				2.22	0.37				
Community$_{forest}$	0.65			0.77				0.33		0.03
Standing dead litter	0.16					1.02			0.06	
Deschampsia nubigena	0.85	0.25		1.30						
Hypochaeris radicata	0.73				0.75	0.50				
Holcus lanatus	0.69		0.45		0.28				0.03	
Rumex acetosella	0.41		0.77							
Leptecophylla tameiameiae	0.42		1.11	1.53						
Sadleria cyatheoides	0.41	1.50			0.14					0.03
Metrosideros polymorpha	0.58		1.43						0.02	
Myrsine lessertiana	0.20		0.39	0.19				1.30		
Ilex anomala	0.42		0.97							0.14
Melicope clusiifolia	0.45	0.53			0.02			0.31		
Cheirodendron trigynum	0.23	0.61				1.11				
Elaphoglossum paleaceum	0.24		0.97					0.28		
Elaphoglossum wawrae	0.36		0.58					0.20		
Lepisorus thunbergianus	0.17	0.80	0.26					0.64		
Bryophytes	0.67			0.84						
Lichen	0.52	0.81			0.40				0.04	

Table 1. Results of non-parametric multiplicative regression (NPMR) distribution models of vegetation around the TWI on windward Haleakala. Forest line models include two types: *binary* = forest or not forest response variable, and *height* = percent cover of the > 5m height class. In addition, forest line models explore two spatial scales: *sub* = a subset of 72 plots that equally bracket the forest line, and *all* = the total n = 136 plots.

We measured the relative importance of each type of predictor variable across all models and found that overall, non-EN climate variables are dominant drivers of vegetation (Fig. 1). We also analyzed the relative importance of each predictor variable and found that relative humidity during EN and slope are as important in some models as any non-EN climate variable (Fig. 2).

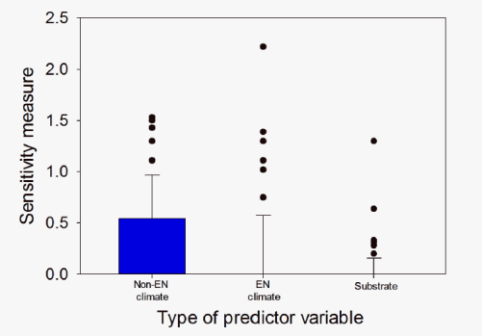

Figure 1. Sensitivity of the model to each of three types of predictor variables for all 24 distribution models, showing all outliers.

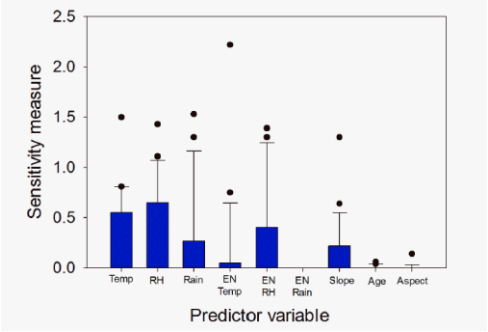

Figure 2. Sensitivity of the model to each predictor variable for all 24 distribution models, showing all outliers.

We tested the robustness of our baseline model of forest line (*sub_binary*, Table 1), which was driven by relative humidity during EN and secondarily by rainfall. To do so, we compared our modeling technique (non-parametric multiplicative regression (NPMR)) to multiple modeling algorithms (boosted regression trees, generalized linear models, multivariate adaptive splines, and random forests). In each of these four models, relative humidity during EN was used to model forest line. In three of the four, it was the most important variable, as in our NPMR model, and in one model it was second in importance to rainfall, similar to our NPMR model. This comparison suggests our modeling results with NPMR are robust.

Spatial scale of the dataset influenced which predictors were chosen to model vegetation. When forest line was modeled with an even design that brackets the forest line with 350' of elevation above and below the ecotone (n = 72), relative humidity during EN is the most important variable and rainfall is a secondary predictor. When the forest line is modeled with our entire vegetation array (n = 136), from alpine grassland to >350' in elevation below forest, relative humidity during EN was again most important, but temperature was a secondary predictor (Table 1; Forest line$_{sub_binary}$ and Forest line$_{all_binary}$).

Future distribution models

For those baseline models driven by rainfall, we modeled future distributions based on PICCC-supported statistical downscaling products (Timm et al. 2014, Fig. 3). We used eight rainfall scenarios to provide a balanced test of vegetation sensitivity to rainfall changes. Changes in rainfall altered the distribution (Fig. 4) and abundance (Table 2, Fig. 5) of vegetation. For example, *D. nubigena* showed downslope movement and significant increase in abundance with reduced rainfall. Forest line position was vulnerable to

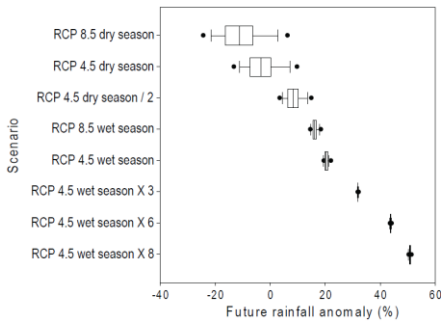

Figure 3. Rainfall anomalies for 8 scenarios used in future vegetation modeling.

changes in rainfall, particularly decreased rainfall. Forest line moved downslope, and forest was lost from nearly 30% of plots with a 10% reduction in rainfall, whereas forest line moved upslope and gained only 15% with a 20% increase (Fig. 6).

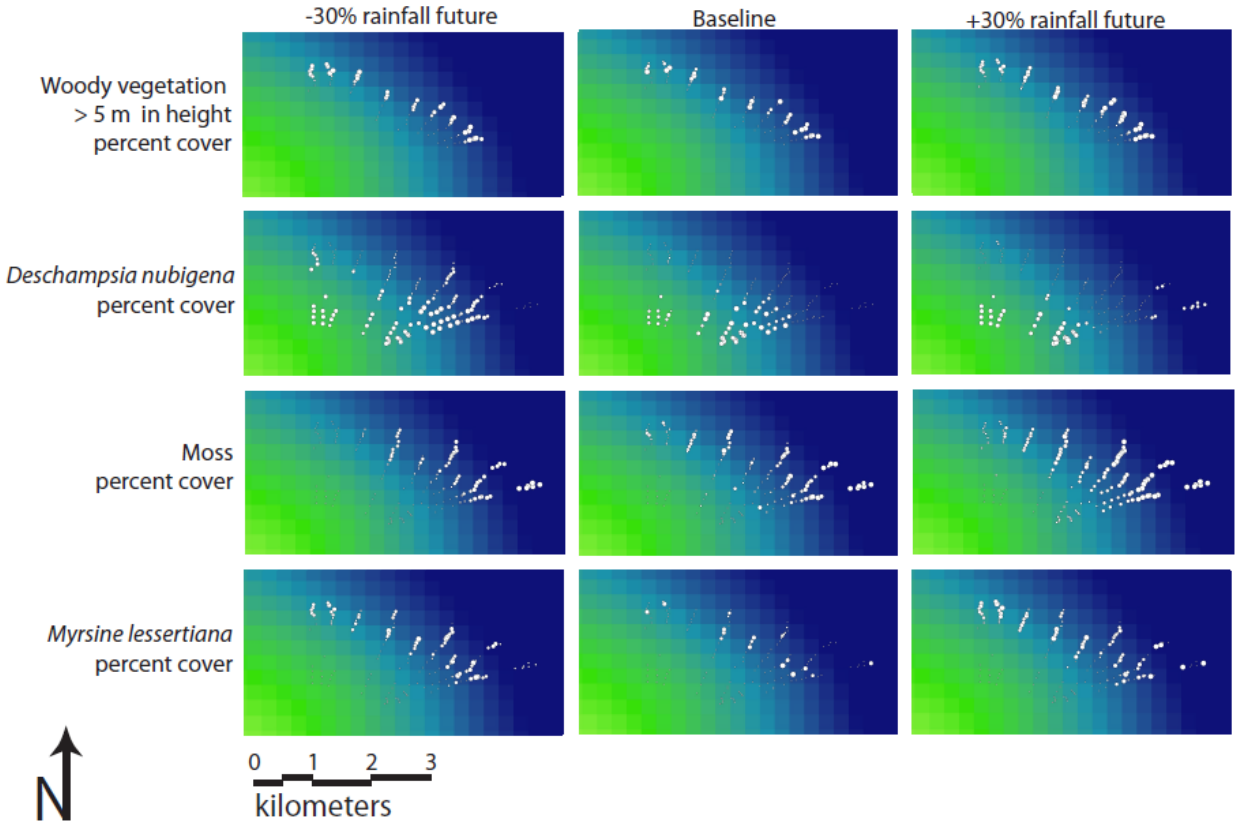

Figure 4. Distribution and abundance of future vegetation around the TWI on Haleakalā against backdrop of mean annual rainfall, from ~ 1700 mm (green) to >8500 mm (blue).

Rainfall scenario	*Deschampsia nubigena*	Moss	*Myrsine lessertiana*	Forest community	>5m height
Baseline	0.17	0.26	0.00	0.03	0.15
RCP 8.5 dry season	0.34**	0.07***	0.02***	-0.84***	0.20*
RCP 4.5 dry season	0.42**	0.11***	0.02***	-0.83***	0.27*
RCP 4.5 dry season / 2	0.21**	0.21***	0.02***	-0.28***	0.40
RCP 4.5 wet season	0.04	0.26	0.02***	0.00	0.45
RCP 8.5 wet season	0.04	0.28**	0.02***	0.22***	0.45
RCP 8.5 wet season X 3	0.03	0.44***	0.02***	0.22***	0.49
RCP 8.5 wet season X 6	0.01	0.55***	0.02***	0.42***	0.50**
RCP 8.5 wet season X 8	0.00	0.61***	0.02***	0.48***	0.57***

Table 2. Wilcoxon signed ranks tests on paired differences in abundance for each of eight rainfall scenarios. Mean abundance is reported and * = $P < 0.05$, ** = $P < 0.005$, *** = $P < 0.001$.

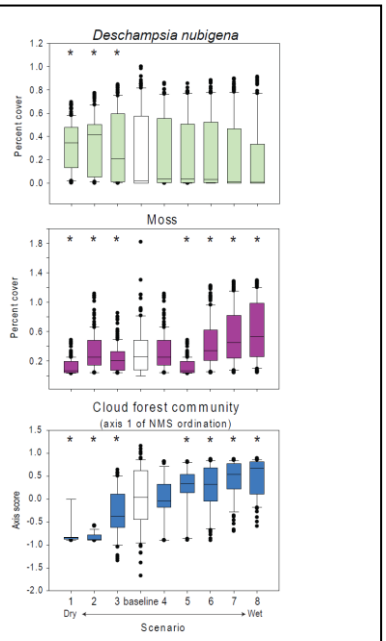

Figure 5. Abundance of vegetation with future rainfall. Significant difference from baseline denoted with *.

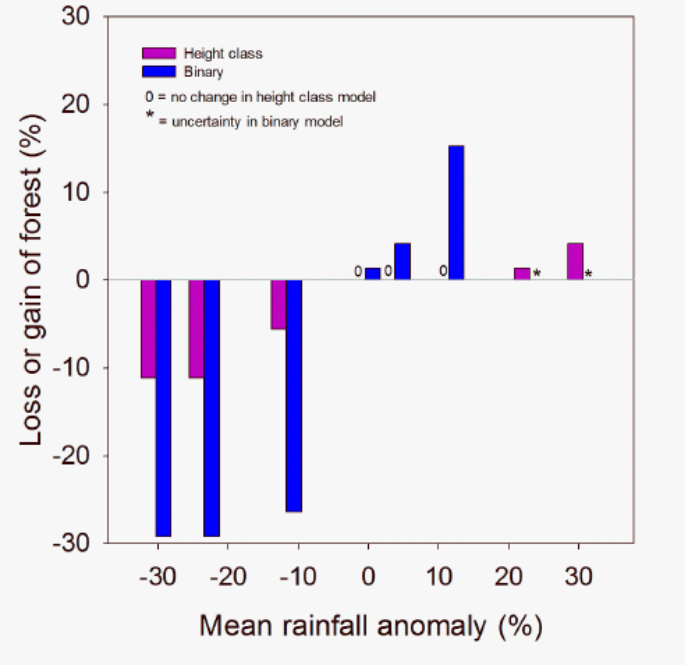

Figure 6. Percent change of forested plots around the forest line with future rainfall scenarios, based on two different forest line models.

Past distribution models

We found that dynamics in the upper limit of cloud forest over the past 3,300 years were driven by onsite moisture variability and the frequency of El Niño. The three paleorecords around the TWI demonstrate that forest line was dynamic over the last three millennia. The cloud forest's upper limit never fell below today's elevation (Fig. 7). However, forest line migrated upslope at least three times over the past 3,250 cal yr BP (calibrated years before present). Forest line was at least 200 m higher than the modern limit from 3250 to 2380 ±100 cal yr BP, again from 1130 to 820 ±100 cal yr BP, and most recently from 470 to 330 ±100 cal yr BP. Changes in forest line elevation are significantly associated ($r^2 = 0.39$) with onsite moisture availability, and secondarily with El Niño frequency and latitudinal position of the ITCZ, which affects tropical rainfall (Fig. 8). The sustained period of lowered forest line from ~ 2,300 to ~ 1,100 cal yr BP occurred during the highest El Niño event-frequency, a time without fire and before Polynesian arrival. Fires did occur above the forest line at least three times in the past – at 100, 320, and 480

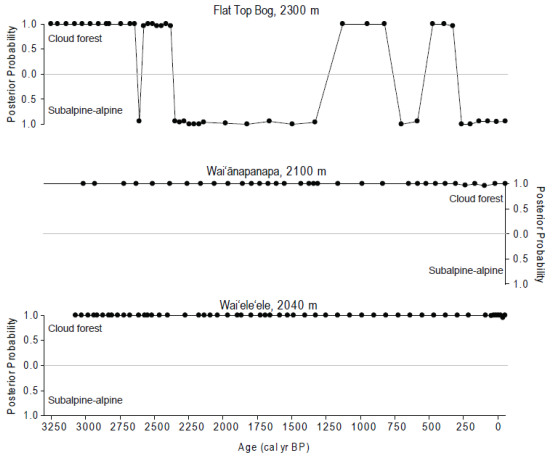

Figure 7. Probability that a fossil pollen sample was derived from a cloud forest or a subalpine-alpine ecosystem for three paleorecords bracketing the TWI on Haleakalā.

years BP. Small fires may have occurred three additional times before those time periods – at 540, 640, and 740 years BP. Whether fires were the result of volcanoes, drought, human land use, or some combination of the three, is difficult to determine from these records. However, evidence for the strong role of El Niño in driving the position of the cloud forest's upper limit – especially with the absence of fire and human impacts – suggests that changes in El Niño or other drivers of moisture availability can control Hawaiian ecosystem dynamics on millennial time scales. These paleoecological data confirm the importance of El Niño to the position of the cloud forest's upper limit, which was suggested by species distribution models of today's forest line position (Crausbay et al., 2014, Oecologia).

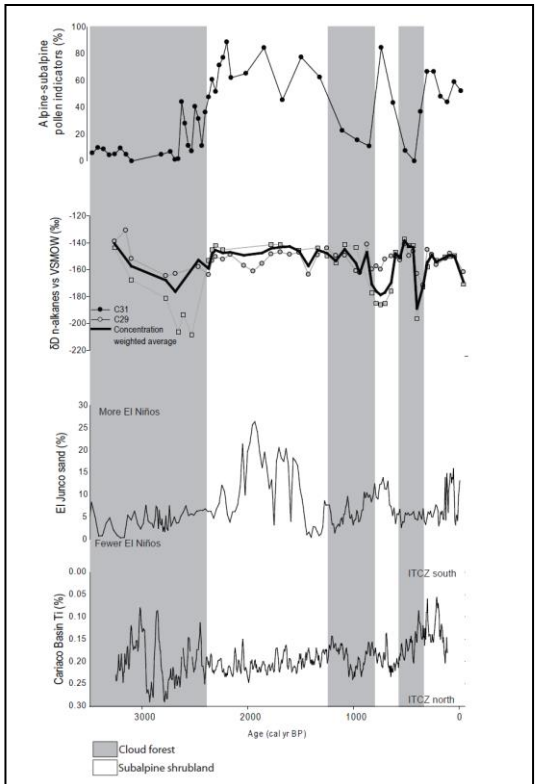

Figure 8. Response (top) and predictor variables that make up an NPMR distribution model of past forest line dynamics. NPMR results: $xR^2 = 0.39$, sensitivity measures: onsite hydrology = 1.3, EN frequency = 0.30, ITCZ = 0.28.

Other paleorecords

We found that the majority of vegetation dynamics over the past 7000 years can be explained by alteration of disturbance regimes (Crausbay et al., 2014, AAAR). The disturbance regime changed at least twice in the paleorecord – first during a time of maximum El Niño frequency around 2300 cal yr BP and again around 500 cal yr BP when a novel fire regime appeared. ACL values show evidence of increased aridity at the onset of both changes in disturbance regimes. These changes were associated with rapid ecological change, evidence for dieback of cloud forest tree taxa, and short-lived increase in vines and lianas. However, the forest's response to drought differed from the response to fire, in terms of species compositio n. Though this cloud forest was dynamic and experienced many disturbances, including dieback events, it has recovered in the past, suggesting a resilient forest when considered over long time scales.

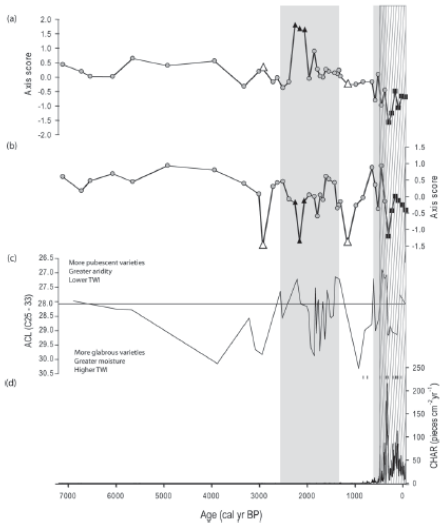

Figure 9. a-b: Changes in vegetation community characteristics over past 7000 years (NMS ordination axes 1 and 2) in response to drought (c) and fire (d).

KEY FINDINGS

Major discoveries

- Moisture is a strong driver of vegetation around the TWI

- Moisture during EN is a strong driver of

vegetation, particularly above the TWI

- Moisture and EN frequency has driven forest line dynamics over the past 3300 years
- Fire occurred on these landscapes, from 850 – 250 cal yrs ago
- Upper cloud forest vegetation over 7000 years changed with drought, fire, and dieback, but was resilient overall.
- Vegetation is sensitive to future changes in rainfall, particularly reduced rainfall
- Downslope movement of vegetation near the TWI is an important scenario for managers to consider.

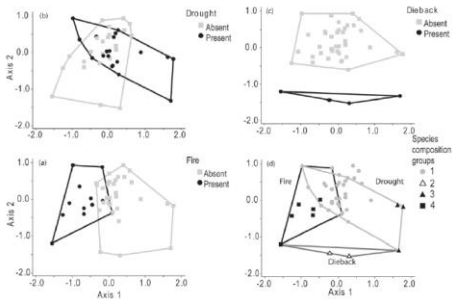

Figure 10. NMS ordination of fossil pollen assemblages over past 7000 years, identified by three different disturbance types (a-c) and major species assemblage groups (d).

Climate-change research is increasingly showing the importance of moisture to ecosystems, suggesting the potential for future changes in moisture to alter ecosystems and potential downslope movement. Also research is increasingly highlighting the role of extreme short-duration climate events, like the EN droughts studied here, in ecosystem dynamics and global change response. This work fits in regionally with work at even higher elevations on the climate change impacts on silverswords (Kruschelnycky et al. 2012). These studies demand a more mechanistic understanding of drought effects on vegetation in Hawai‘i and an exploration of the role of carbon starvation, and or cavitation, with moisture stress. Our research also clearly highlights a need for greater skill in predicting the future of EN.

Management applications

Our research shows that vegetation is sensitive to moisture, especially reduced moisture. Our future modeling suggests the possibility of downslope movement of forest with reduced rainfall. Downslope movement of cloud forest and the tussock grass *D. nubigena*, coupled with a temperature-driven upslope movement in avian malaria is an important scenario for endangered forest bird and nene management.

Our research also shows that vegetation is sensitive to EN, especially at higher elevations just above the TWI. This pattern suggests managers may benefit from scenarios of extreme drought events causing rapid vegetation change in subalpine and alpine areas.

Our paleorecords show that fires burned in the subalpine and alpine areas, starting around 850 years ago, long after Polynesian arrival. Fire occurrence is associated with evidence for drought in our paleorecords, however ignition source (human or natural) remains unclear. Including a scenario for fire in these high elevation landscapes may be useful to avoid a fire-related ecological surprise.

CONCLUSIONS AND RECOMMENDATIONS

Project progression

In hindsight, I would have used both *dynamical* and *statistical* downscaling for future vegetation models, in order to capture future changes in temperature and relative humidity. In addition, the future of El Niño is too uncertain to complete future modeling for vegetation types driven by EN, especially the forest line, where we could leverage the long time span afforded by the paleo-distribution models. Highlighting the role of EN in baseline models leads to many more questions. What aspects of EN affect vegetation – frequency or intensity? By what mechanism does EN affect vegetation patterns from forest line to species distributions in subalpine and alpine ecosystems? What is the physiological response of these species to strong drought?

Recommended next steps

- The role of EN in vegetation patterns at and above the TWI (forest line, subalpine shrubland, alpine grassland)
- The relationship between EN and the TWI in terms of microclimate
- Physiological response of different species to drought
- The paleo-fire regime in ecosystems above the TWI
- The future of EN frequency and intensity
- The future of TWI frequency and mean base height

Conservation decisions

Managers may benefit from (1) anticipating downslope movement of the upper forests and (2) revisiting management decisions based on the assumption of upslope movement of forest.

OUTREACH

None to report.

SCIENCE OUTPUTS

Publications

Crausbay S., Genderjahn, S., Hotchkiss, S., Sachse, D., Kahmen, A., and Arndt, S. 2014. Vegetation dynamics at the upper reaches of a tropical montane forest are driven by fire and drought over the past 7300 years. Arctic, Antarctic, and Alpine Research 46:787-799

Crausbay S., Frazier A., Giambelluca T., Longman R., and Hotchkiss S. 2014. Moisture status during a strong El Niño explains a tropical montane cloud forest's upper limit. Oecologia 175:273-284

Publications in preparation

Crausbay S., Hotchkiss S., Sachse D., and Kamen A. A tropical forest ecotone tracked changes in El Niño frequency for the past 3300 years. in preparation for Proceedings of the National Academy of Sciences (USA)

Oral presentations

Crausbay S., Frazier A., Hotchkiss S., and Giambelluca, T. 2015. Past, present and future distribution of the cloud forest's upper limit in Haleakalā National Park: the importance of moisture and El Niño-induced drought. *Science for Parks, Parks for Science*, Berkeley, CA (to be presented March 27, 2015)

Crausbay S., Hotchkiss S. and Martin P. 2014. Contrasting tropical montane vegetation dynamics in the Pacific and Caribbean over the late Holocene. *Island Biology*, Honolulu, HI

Crausbay, S.D., and S.C. Hotchkiss. 2013. Little HaleNet: climate and vegetation at a landscape scale. *HaleNet 25th Anniversary Symposium*, Honolulu, HI

Crausbay, S.D., and S.C. Hotchkiss. 2013. The past as prologue: Using present distributions and past dynamics to inform future scenarios for high-elevation vegetation, *PICSC-PICCC Climate Science Symposium*, Honolulu, HI

Crausbay, S.D., and S.C. Hotchkiss. 2013. What are we doing modeling the future? *Hawaii Ecosystems Meeting*, Hilo, HI

Crausbay S. and Hotchkiss S. 2012. Vegetation dynamics at the upper reaches of a tropical montane cloud forest are driven by ENSO and fire. *Vulnerable Islands in the Sky: Science & Management of Tropical Alpine & Sub-alpine Ecosystems*, Waimea, HI

Crausbay S. and Hotchkiss S. 2012. Moisture and El Niño Drive Cloud Forest Community Composition and Upper Limit on Haleakalā. *Hawaii Conservation Conference,* Honolulu, HI

Crausbay S. and Hotchkiss S. 2011. Dynamics of a tropical forest ecotone in Hawaii are driven by changes in large scale climate features and fire. *Ecological Society of America*, Austin, TX

Crausbay S. and Hotchkiss S. 2011. Vegetation dynamics at the upper reaches of a tropical montane cloud forest are driven by ENSO and fire. *Holocene Paleoclimate in the Hawaiian Islands and its Large-scale Context,* Kilauea Military Camp, HI

Giambelluca T., Crausbay S., Hotchkiss S., Gotsch S., Frazier A, Longman R. 2014. Drought as a determinant of tropical montane forest line position. *American Geophysical Union*, San Francisco, CA

Giambelluca T., Crausbay S., Krushelnycky P., Loope L., Nullet M., Longman R., Hotchkiss S. and Frazier A. 2014. Evidence of climate change and ecosystem response at Hawai‘i’s high-elevation forest-shrubland ecotone. *Mountain Observatories*, Reno, NV